Acta Materialia Turcica

Volume 5, September 2021, Pages 11-17

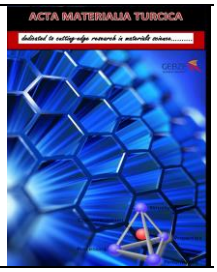

Non-linear Analysis of Deformation Behavior of HA/PLCL Porous Bio-composites

F. H. M. AZAHAR [a,b,c*], M. TODO[b,c], N. A. N. IZMIN[b,c]

[a]*Kyushu University Program for Leading Graduate School, Green Asia Education Center, Interdisciplinary Graduate School of Engineering Sciences, Kyushu University, Fukuoka, Japan.*
[b]*Research Institute for Applied Mechanics (RIAM), Kyushu University, Fukuoka, Japan*
[c]*Department of Molecular and Material Sciences, Kyushu University, Fukuoka, Japan.*
** Corresponding author: mohamad.azahar.519@s.kyushu-u.ac.jp*

Abstract:

It is well-known that the biology of bone mainly consists of the inorganic minerals, therefore bioceramics with similar constituent to that inorganic minerals of bone, e.g., hydroxyapatite [$Ca_{10}(PO_4)_6(OH)_2$] (HA) are extensively used for the scaffold fabrication. Recently, biodegradable synthetic polymers (biopolymer) are commonly used as composite materials to enhance the mechanical properties of pure HA porous scaffold. In this work, HA based scaffold incorporated biopolymer namely, Poly(L-Lactide-co-ε-Caprolactone) (PLCL) is developed in an attempt to overcome the brittleness of pure HA scaffold. Further, two theoretical models are developed to express the non-linearity of the load-displacement curve obtained from the three-point bending test. Finally, the surface morphology of this material is observed using the Scanning Electron Microscopy (SEM). HA/PLCL material is observed to have a non-linear deformation where Model II depicts better accuracy compared to Model I with 9.6% RMS error while 11.61% RMS error for Model I. Due to the overestimation values given by Model I, Model II seems to have a better prediction on the load-displacement curve. The morphological structure of HA/PLCL shows two layers of interconnecting pores where the addition of polymer has enhanced the mechanical properties by providing ductility.

Keywords: Biomaterials; Nonlinear; Deformation; PLCL; Porous.

1. INTRODUCTION

In recent years, the development of porous bioceramics scaffolds such as hydroxyapatite (HA), has seen massive advancement in regenerative medicine due to their demand for being stronger, biocompatibility, bioactivity and non-toxicity [1]–[6]. From the mechanical perspective, ideally, a scaffold should possess sufficient mechanical properties which could mimic the mechanical properties of the cancellous bone or the target tissue. However, a scaffold fabricated with hydroxyapatite alone would provide a major disadvantage, in which this material is known to be brittle in nature with low strength. Hence, biodegradable synthetic polymers such as poly (ε-caprolactone) (PCL), poly (L-lactic acid) (PLLA) and collagen type I are commonly used as composite materials to overcome this problem by adding flexibility to the structures [7]–[10]. In addition, it is important for a scaffold to have a high porosity and good interconnectivity between pores to allow osteoconductivity, nutrient transport as well as to permit cell adhesion [11], [12]. Therefore, suitable biomaterials and proper techniques have to be carefully selected for the fabrication of scaffolds. In order to predict the mechanical behavior of the scaffold, it is common that the scaffold undergoes mechanical test

Corresponding Author E-mail: *mohamad.azahar.519@s.kyushu-u.ac.jp*

Acta Materialia Turcica

Volume 5, September 2021, Pages 11-17

such as compression and bending test. As such, Huang et al. [13] developed a polymer-ceramic composite scaffold and investigate the effects of different bioceramics materials i.e. hydroxyapatite and β-tricalcium phosphate reinforced with PCL, using the extrusion-based additive manufacturing system technique. It is reported that better biological properties were obtained by scaffold containing HA while β-TCP provided better mechanical properties. Another interesting work from Phanny et al. [14], where the novel polymeric secondary phase was introduced in the fabrication of HA/PCL and HA/PLLA scaffold. Their compressive mechanical properties were assessed and compared with the pure coated HA/PCL and HA/PLLA scaffold (without the polymeric secondary phase). The result showed that there was an improvement on the mechanical properties of the two-phase scaffold compared to the coated scaffold. It was also reported that the spongy polymer structure has provided flexibility thus preserved the whole structure from brittle fracture. On another note, research works focusing on the development of theoretical model to express the linear and non-linear deformation behavior has been gaining attention. For example, a linear elasticity model was presented by Ju et al. [15] to fit the load-displacement curve and was comparable to the published literature. In this work, we developed a HA based scaffold incorporating Poly(L-Lactide-co-ε-Caprolactone) (PLCL), focusing in the enhancement of the mechanical properties of the scaffold material. A beam type scaffold is introduced in this study to determine the mechanical properties of the scaffold by conducting the 3-point bending test. Further, the load-displacement relationship is expressed through the development of two theoretical models to predict the non-linear deformation behavior of the material. Finally, the integration of HA material to the biopolymers matrix is analyzed using the scanning electron microscopy (SEM) machine where the typical surface morphology is presented.

1.1. Non-Linear Deformation Model

Model I

The mechanical behavior of a composite biomaterial scaffold is best understood using the theoretical models, where the analysis of the deformation is possible. For fully describing the deformation of a beam, it is necessary to consider a simply supported beam at both ends subjected to a concentrated load, P (see Figure 1). All of the parameters for the expression of displacement, δ are denoted as L, H, B, P, c, υ, and x, describing the half-length of the beam from the support span, thickness of the beam, width of the beam, load applied to the beam, the length of plastic deformation region, displacement in y-direction and displacement in x-direction, respectively. The stress-strain relationship of the material is first assumed to be all non-linear, thus Hollomon's equation is employed where it is characterized by an exponential function with F and n are the variable index as shown in Figure 2.

$$\sigma = F\varepsilon^{n} \tag{1}$$

Then the loading-point displacement δ of the three-point bending beam is given by:

$$\delta = KP^{1/n}[n(L-x)^{(2n+1)}+(2n+1)L^{(n+1)/n}x-nL^{(2n+1)/n}] \tag{2}$$

where, $K = \left[\dfrac{n(n+2)2^{n}}{(n+1)(2n+1)H^{n+2}BF}\right]^{1/n}$, P refers to the applied load (N), x is the horizontal distance at any location along the beam, H is the height of the beam, B is the width of the beam, and F and n are the strength coefficient (N.mm^{-2}) and the strain hardening exponent, respectively. It is important to note that L used in the equation is the half-length of the beam from support span (in this case, L=10mm).

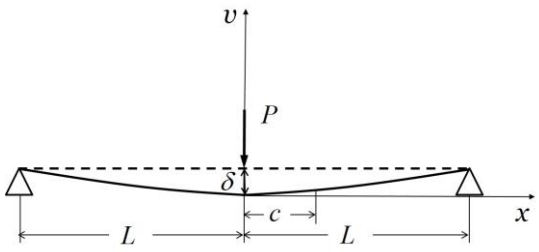

Figure 1. Bending deformation of a simply supported non-linear beam.

Corresponding Author E-mail: *mohamad.azahar.519@s.kyushu-u.ac.jp*

Acta Materialia Turcica

Volume 5, September 2021, Pages 11-17

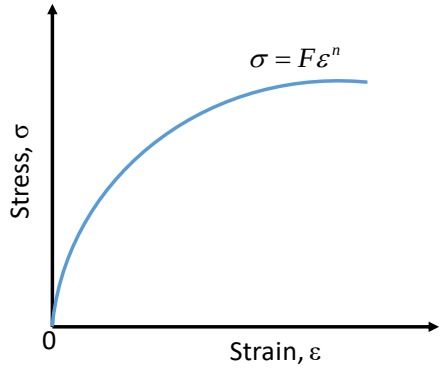

Figure 2. Non-linear stress-strain relationship.

Model II

In model II, the material is assumed to behave as elastic-plastic as shown in Figure 3, where the Euler-Bernoulli (E-B) beam theory and Ludwik's equation are adopted. The theoretical analysis is first divided into two regions, i.e. elastic and plastic region. For the elastic region, the material is assumed to behave as linear elastic and obeys the Hooke's Law;

$$\sigma = E\varepsilon \tag{3}$$

where σ is the stress (MPa), E is the elastic modulus (N.mm^{-2}), while ε refers to the strain. Therefore, no inelastic irreversibility accounted during this stage. The differential equation for the elastic curve of a beam is generally expressed in terms of bending moment, M and is given by,

$$EI\frac{d^2y}{dx^2} = M(x) \tag{4}$$

Here, I is the moment of inertia (mm^4), and the product of EI refers to the rigidity of the material, while the term $\frac{d^2y}{dx^2}$ is the second derivative of the bending deformation.

Hence, the relationship between load, P and the loading-point deformation, δ, for the elastic region *(0≤ P ≤ Py)* may be written as,

$$\delta_e = \frac{PL^3}{6EI} \tag{5}$$

Again, L used in the equation is the half length of the beam from the support span (mm), and subscript e refers to the elastic region. The elastic modulus, E was determined from the initial gradient of the load-deformation curve, m with b and h denote the beam width and thickness, respectively. The equation follows the *ASTM D7264* standard method *Procedure A* [16]:

$$E = \frac{(2L)^3 m}{4bh^3} \tag{6}$$

For the plastic region, Ludwik's equation is then employed, as can be seen in Figure 4. Recall that for elastic region, the material is assumed to behave as linear elastic and Euler-Bernoulli's theorem is used to form the equation. General wisdom is that most polymeric materials undergo plasticity before fracture, hence it is customary to invoke the strain hardening coefficients to predict the plastic deformation. In contrast to Hollomon's equation, one significant feature of the Ludwik's equation is the addition of yield stress, σ_y that gives the continuation from elastic to plastic region. Therefore, the deformation for plastic region is obtained as,

$$\delta_p = KP^{1/n}[n(L-x)^{(2n+1)} + (2n+1)L^{(n+1)/n}x - nL^{(2n+1)/n}] + \delta_y \tag{7}$$

where, $K = \left[\frac{n(n+2)2^n}{(n+1)(2n+1)h^{n+2}bF}\right]^{1/n}$ and δy refers to the deformation at the yield load of elastic region and calculated using Equation 5.

Corresponding Author E-mail: *mohamad.azahar.519@s.kyushu-u.ac.jp*

Acta Materialia Turcica

Volume 5, September 2021, Pages 11-17

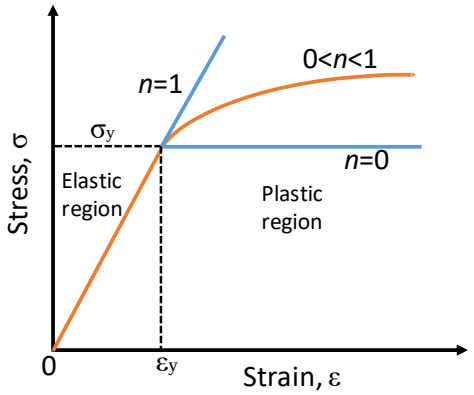

Figure 3. Model II: Improved model for elastic and plastic region.

2. EXPERIMENTAL PROCEDURE

2.1. Fabrication

In order to obtain the porous structure of scaffold with three-dimensional fully interconnecting pores, the HA porous material was first fabricated by employing the template method. The slurry of HA material was prepared by mixing the commercial PS-1, Sangi Co, Ltd. micro-HA powder (particle size ranging from 0.03μm to 0.1μm) with 5wt% polyvinyl alcohol (PVA) [CH_2CHOH_n] from Wako Pure Chemical Industries, Ltd. This HA/PVA were mixed with a ratio of 5:7 for a total duration of 12 minutes (8 minutes kneading, 4 minutes degassing) using the centrifuge mixing machine from Imoto Co, Ltd. Next, PU sponge was cut into beam shaped of 10 mm x 10 mm x 70 mm dimensions, and immersed in the HA slurry. The excess slurry was then removed from the sponge template by applying full compression on it with glass plates. The slurry coated sponge was dried at room temperature for 48 hours. Next, the dried sponge went for the calcination process at 400°C for 6 hours to burn out the binder (PVA) and sponge template with heating rate of 10°C / min, followed by the sintering process at 1300°C for another 4 hours for the solidification of HA porous scaffold. Biodegradable synthetic polymers namely, poly Poly(L-Lactide-co-ε-Caprolactone) (PLCL) was employed to reinforce the HA porous scaffold by coating and using the freeze-drying method. Firstly, the commercial PLCL pellets were dissolved into 50ml 1,4-dioxane solution (Kishida Chemical Co., Ltd.) to obtain a 3wt% solution concentration and it was stirred at 80°C, 320 rpm overnight. The HA porous scaffold was then dipped into the PLCL solution and vacuumed using the vacuum sputter machine for 1 hour to ensure the complete removal of air. The soaked HA scaffold was put on the sample plate and froze for 24 hours at -80°C. Finally, the frozen HA/PLCL porous scaffold was freeze dried at -50°C for another 24 hours.

2.2. Microstructure characterization and mechanical test

The three-point bending test was conducted using the Shimadzu Compact Tabletop Testing Machine EZTest (EZ-S Series) with 10N load cell. This three-point bending test provided significant values for the load-displacement relationship, which determined the mechanical behavior of the scaffold. The morphology of the fabricated scaffold was evaluated using the scanning electron microscopy (SEM).

Since the fabricated scaffolds are porous materials, porosity is one of the important properties to be considered. In this work, porosity was determined by using the following equation:

$$Porosity(\%) = \frac{w_3 - w_1}{w_3 - w_2} \times 100 \quad (8)$$

where W_1 denotes the weight of the dry sample, W_2 refers to the weight of the sample in ethanol and W_3 is the weight of wet sample soaked with ethanol. The Archimedes principle was adopted in determining W_2 and ethanol was used to measure the fluid displacement since ethanol is less dense than the composite material. The average pore size (Feret's diameter, x_F) of the material was then calculated using ImageJ Software.

3. RESULTS AND DISCUSSION

The SEM morphological structure of HA/PLCL porous scaffold is shown in Figure 4. The scaffold produced a well-developed interconnecting pore structure, with two types of architectural pore arrangement, (i) initial pore formed by the HA structure, and (ii) honeycomb-like PLCL pore structure created due to the freeze-drying process which strengthen the mechanical properties of the scaffold. The average pore size and porosity were approximately 500-700μm and

Corresponding Author E-mail: *mohamad.azahar.519@s.kyushu-u.ac.jp*

Acta Materialia Turcica

Volume 5, September 2021, Pages 11-17

82%, respectively (see Table 1). Figure 5 illustrates the experimental load-displacement curve of HA/PLCL obtained from the three-point bending test, where it is confirmed that this material exhibits non-linear deformation. The load increased linearly showing the linear-elastic behavior, up to the yield point where the initiation of crack occurred at the HA framework (the large interconnecting pore). Nonetheless, the addition of polymer material (PLCL) has strengthen the HA structure by providing ductile property, thus creating a plastic deformation ligament. This slightly flattens the load-displacement curve after the yield point and increases uniformly due to the cell walls of HA and polymer that collapse before it completely fractured approximately at the displacement of 6.5mm. Since the experimental curve is too complex to represent its mechanical behavior, thus it is best understood using the stress-strain relationship. Two theoretical models i.e. Model I and Model II were first validated using values adopted from the experimental work. The deformation at various loads is calculated for each model and their fitting accuracies are compared. Table 2 gives the summary of the best fit coefficients for HA/PLCL beam, and Figure 6 shows the model fittings. It can be seen that Model II provides superior fitting accuracy compared tothe fitting by Model I. For the deformation at the elastic region, overestimation values is given by Model I, hitherto, both models provide almost similar deformation values during the plastic region (>1.87). This is due to the significance of strain hardening coefficients which is invoked in both models. Therefore, it could be confirmed that the infinite slope assumption given by Hollomon's equation leads to the overestimation at the elastic region. It is also interesting to note that the addition of δ_y term in Model III has its profound effect in providing the connection between the elastic and plastic region, thus giving a better accuracy.

Table 1. Microstructure properties of HA/PLCL.

Microstructure properties	HA / PLCL
Average inner pore size (μm)	68.05
Average outer pore size (μm)	479.77
Polymer concentration (wt%)	3.0
Porosity (%)	92.28

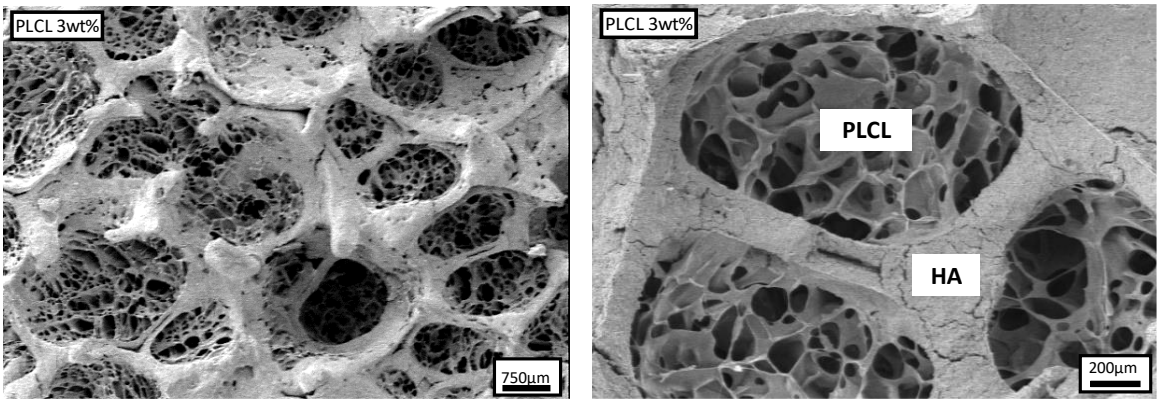

Figure 4. HA/PLCL microstructure.

Corresponding Author E-mail: *mohamad.azahar.519@s.kyushu-u.ac.jp*

Acta Materialia Turcica

Volume 3, June 2019, Pages 1-7

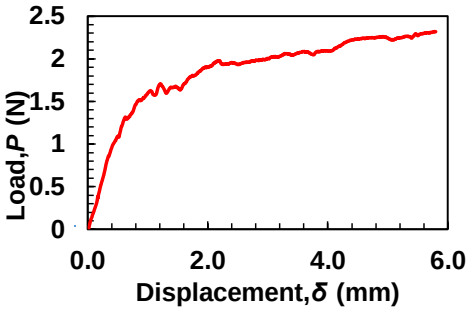

Figure 5 Load-displacement curve.

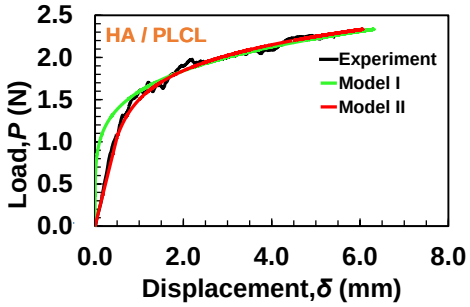

Figure 6. Model fitting.

Table 2. Best fit coefficients for model fitting.

Fitting parameters	HA/PLCL	
	Model I	**Model II**
b (mm)	7.6	
h (mm)	6.6	
L (mm)	10	
E (MPa)	1.935	
P_y (N)	N/A	1.09
n (-)	0.21	0.16
F (MPa)	0.03	0.02
x (mm)	10	10
Error (%)	11.81	9.6

4. CONCLUSION

The structural stability of brittle HA and its mechanical properties has been improved by introducing PLCL polymer using the polymeric secondary phase fabrication method. It is found that the porous structure of HA/PLCL contains two types of arrangement namely, the initial HA interconnecting porous structure and the honeycomb like PLCL layer within the HA pores. The scaffold was able to provide porosity and average outer pore size more than 80% and 400µm, respectively, which is ideal for cell adhesion and nutrient transport. However, the average pore size obtained for both scaffold's inner pores are lower than 100µm, mainly due to the polymer concentration and molecular weight. Theoretical models were developed to predict the deformation behavior of the scaffold addressing the linear and non-linear behavior whilst the variation in strain hardening is accounted for. Each model was first validated using the experimental data in which their fitting accuracies were calculated using regression method and compared. It was found that Model II gives up to 92.96% accuracy while the accuracy given by Model I was 88.18%.

5. ACKNOWLEDGEMENT

The author would like to thank the Green Asia Program for Leading Graduate School, Kyushu University for the financial support and Research Institute for Applies Mechanics, Kyushu University for the facilities provided to conduct this study.

6. REFERENCES

[1] D. W. Hutmacher and A. J. Garcia, "Scaffold-based bone engineering by using genetically modified cells," *Gene*, vol. 347, no. 1. Elsevier, pp. 1–10, Feb. 28, 2005, doi: 10.1016/j.gene.2004.12.040.

[2] A. G. Mikos and J. S. Temenoff, "Formation of highly porous biodegradable scaffolds for tissue engineering," *Electronic Journal of Biotechnology*, vol. 3, no. 2, pp. 114–119, 2000, doi: 10.2225/vol3-issue2-fulltext-5.

[3] M. C. Hacker and A. G. Mikos, "Trends in Tissue

Corresponding Author E-mail: yboztoprak@marmara.edu.tr

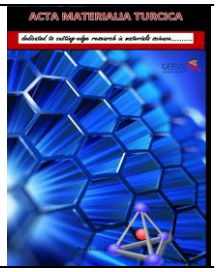

Engineering Research," *Tissue Engineering*, vol. 12, no. 8, pp. 2049–2057, 2006, doi: 10.1089/ten.2006.12.2049.

[4] A. J. Salgado, O. P. Coutinho, and R. L. Reis, "Bone tissue engineering: State of the art and future trends," *Macromolecular Bioscience*, vol. 4, no. 8, pp. 743–765, 2004, doi: 10.1002/mabi.200400026.

[5] M. Todo, J. E. Park, H. Kuraoka, J. W. Kim, K. Taki, and M. Ohshima, "Compressive deformation behavior of porous PLLA/PCL polymer blend," *Journal of Materials Science*, vol. 44, no. 15, pp. 4191–4194, 2009, doi: 10.1007/s10853-009-3546-0.

[6] M. Todo, P. Yos, T. Arahira, and A. Myoui, "Development and characterization of porous hydroxyapatite scaffolds reinforced with polymeric secondary phase for bone tissue engineering," *Biomaterials and Tissue Technology*, vol. 2, no. 1, pp. 1–8, 2018.

[7] M. C. Azevedo, R. L. REIS, M. B. Claase, D. W. Grijpma, and J. Feijen, "Development and properties of polycaprolactone/hydroxyapatite composite biomaterials," *Journal of Material Science. Material in Medicine*, vol. 14, no. 2, pp. 103–107, 2003.

[8] V. Guarino *et al.*, "The role of hydroxyapatite as solid signal on performance of PCL porous scaffolds for bone tissue regeneration," *Journal of Biomedical Materials Research Part B : Applied Biomaterials*, vol. 86B, no. 2, pp. 548–557, 2008.

[9] H.-W. Kim, Jonathan C. Knowles, and Hyoun-Ee Kim, "Hydroxtapatite/poly (e-caprolactone) composite coatings on hydroxyapatite porous bone scaffold for drug delivery," *Biomaterials*, vol. 25, no. 7–8, pp. 1279–1287, 2004.

[10] V. Mourinno and A. R. Boccaccini, "Bone tissue engineering therapeutics-controlled drug delivery in three dimensional scaffolds," *Journal of the Royal Society Interface*, vol. 7, no. 43, pp. 209–227, 2010.

[11] S. Levenberg and R. Langer, "Advances in Tissue Engineering," *Current Topics in Developmental Biology*, vol. 61, pp. 113–134, Jan. 2004, doi: 10.1016/S0070-2153(04)61005-2.

[12] R. Langer and J. Vacanti, "Tissue Engineering," *Science*, vol. 260, no. 5110, pp. 920–926, 1993.

[13] B. Huang, G. Caetano, C. Vyas, J. J. Blaker, C. Diver, and P. Bártolo, "Polymer-ceramic composite scaffolds: The effect of hydroxyapatite and β-tri-calcium phosphate," *Materials*, vol. 11, no. 1, 2018, doi: 10.3390/ma11010129.

[14] Y. Phanny and M. Todo, "Development and characterization of poly(ε-caprolactone) reinforced porous hydroxyapatite for bone tissue engineering," *Key Engineering Materials*, vol. 529–530, no. 1, pp. 447–452, 2013.

[15] B. F. Ju, K. T. Wan, and K. K. Liu, "Indentation of a square elastomeric thin film by a flat-ended cylindrical punch in the presence of long-range intersurface forces," *Journal of Applied Physics*, vol. 96, no. 11, pp. 6159–6163, 2004, doi: 10.1063/1.1812822.

[16] ASTM International, "Astm Designation: D 7264/D 7264M-07 Standard Test Method for Flexural Properties of Polymer Matrix Composite Materials," *Annual Book of ASTM Standards*, vol. i, no. C, pp. 1–11, 2007, doi: 10.1520/D7264.

Corresponding Author E-mail: *mohamad.azahar.519@s.kyushu-u.ac.jp*